

Designing Modular Series-Elastic Actuators for Safe Human-Robot Collaboration in Industrial Settings

José de Gea Fernández, Holger Sprengel, Martin Mallwitz, Michael Zipper, Bingbin Yu

*DFKI, Robotics Innovation Center,
Bremen, 28359, Germany*

**E-mail: jose.de_gea_fernandez@dfki.de*

Vinzenz Bargsten

*University of Bremen, Robotics Research Group,
Bremen, 28359, Germany*

This article describes the design of new modular series-elastic actuators within the European project FourByThree which will serve as basis to build robot manipulators of different morphology.

Keywords: series-elastic actuators, human-robot collaboration, modularity, safety

1. Introduction

Until recently, most industrial robots were confined behind a cage, moving at high-speeds and with sub-millimeter precision. Given the danger of a collision with such (usually) huge and heavy robots, if a person enters the workspace of the robot, external sensor systems will detect the intrusion and stop the robot to avoid accidents. However, this situation has been changing in recent years.¹ There are currently many commercially-available examples of a new generation of robots which allow physical contact between human and robots. One example is the robot Baxter (and Sawyer),² whose motors incorporate in series an elastic element (mechanical spring) which ensures that even in case of software malfunctioning or power failure, the robot would remain always flexible (soft) to the external contact. Another example are the robots developed by Universal Robots³ which look externally like traditional industrial robots but are certifiable for most human-robot collaborative tasks. Those robots include several safety measures, among others, the limitation of the maximum forces. Probably the

most well-known example of lightweight robot for human-robot collaboration are the KUKA LBR iiwa robots.⁴ Those include joint torque sensors which enable the possibility of accurate dynamic control and, additionally, collision detection.

In the current project FourByThree, the aim was to combine two of the concepts used in the previous robots: active compliance control (in this case, use of dynamic models and monitoring of motor currents to estimate joint torques) and the use of passive elastic elements to provide safety against collisions while, at the same time, providing a second source of torque estimation.

2. Actuator Mechanics

Actuators are a central element in the project, as they allow creating the modular concept and offer some of the functionalities needed in the safety strategy, i.e. speed, force and torque monitoring. It was initially decided to build three different actuator sizes (with torques 28 Nm, 50 Nm, and 120 Nm, respectively, at link side). The initial list of requirements contemplated among others:

- Maximum link-side torques M_{max} : 28Nm, 50Nm and 120Nm
- Mechanical deflection $\phi = \pm 5$ deg at M_{max}
- Compact, modular and lightweight design
- Link-side speed $n_{max} = 15rpm$
- Safety brake



Fig. 1. *left*: Assembled 28Nm Actuator, *right*: elastic element based on spring discs

At the time of writing this paper, two actuators have been built: the ones with torques 28Nm and 50Nm. The design of the third one, 120Nm,

is currently being finished. All actuators are based on previous modular actuators designed at DFKI.^{5,6} The actuators combine Robodrive brushless DC motors with Harmonic Drive gears. Additionally, in-house developed motor electronics consisting of four PCBs is embedded in each actuator.

Type	I	II
Repetitive Torque (Nm)	25	50
Stiffness (Nm/rad)	175	570
Gear Ratio	100	120
Weight (kg)	0,6	2,5

Fig. 2. Mechanical features of the designed actuators

To develop the 28Nm-actuator, the previous developments of the project CAPIO⁷ - which were already using an elastic element - were taken as starting point. In this case, the elastic element is made of a combination of small disc springs which are at both sides of a lever rotating with the motor (see Fig.1). A re-design was required to accommodate for: embedded electronics entirely based on FPGA as computational unit (previously was a hybrid solution using a microcontroller and a FPGA), several mechanical optimizations to ease the actuator assembly, and the introduction of the so-called 'E-brake': a fourth electronics board as 'Electronic-brake' (details in Section 3). The main characteristics of the actuator are summarized in Table 2.

To develop the 50Nm-actuator, a new spring element based on coil springs has been developed. The spring coupling has a progressive characteristic: initially it exhibits a linear characteristic until approx. 5 degrees of deflection with the desired stiffness, and after that, a more abrupt increase of stiffness is introduced. The idea is to avoid that the spring completely compresses at the maximum torque, but instead, it gets stiffer. The solution is to use a second stiffer spring placed inside the 'main' spring. That second spring only starts affecting the response after 5 degrees of compression.

3. Embedded Electronics

As previously mentioned, the embedded electronics is based on previous designs at DFKI. The usual electronics is composed of three PCBs which incorporate all sensors that are required to monitor and control the actuators. Three motor current sensors are integrated in the low phases of the



Fig. 3. *left*: Assembled 50Nm Actuator, *right*: elastic element based on coil springs

three-phase H-bridges. Absolute encoders with 19-bit resolution before and after the gear measure the motor position. Additionally, in these actuators, a third absolute encoder is placed after the elastic element (link position). The interface to high-level control units is realised via a LVDS bus with an in-house developed communication protocol (Node-level Data Link Communication (NDLCom⁸)). All mentioned sensors as well as current, speed, and position controllers are processed by a Spartan6 FPGA from Xilinx.

Additionally, the actuator electronics has been enhanced in this project with two additional electronic boards: a board for enabling/disabling the mechanical brakes of the 50 Nm actuators (the so-called 'BrakeBoard') which additionally also monitors the motor phase currents as a redundant motor current measurement, and a board for short-circuiting the motor phases of the 28Nm actuators (the so-called 'E-brake') and use that effect as electrical brake. More details about them will follow in the next sections.

The stack of electronics of the 50Nm actuator (the electronics of the 28Nm actuator is similar, but exchanging the 'BrakeBoard' for a 'E-Board') is composed of:

- BrakeBoard. It is in charge of controlling the mechanical brake and used as an additional measurement of the motor currents.
- FPGA Board. It includes a Spartan6 FPGA and peripherals to perform all the required actuator control.
- Power Board. Connects the board to the motor phases, includes the motor drivers and motor current measurements (low-side of the H-bridges).
- Connection Board. Includes communication drivers and position

sensors, signal conditioning and required connectors.

3.1. *BrakeBoard*

The 50 Nm actuators include a safety mechanical brake (Kendrion permanent-magnet with a maximum transmissible torque of 3Nm) and thus a new electronics PCB (the 'Brakeboard') was designed to control it. The BrakeBoard includes the required control electronics to keep the brake open while the motor power is ON. Moreover, the microcontroller on the board is additionally used to measure the motor phase currents. Those measurements will be sent to the FPGA to be compared with the additional motor current measurements available from other sources (motor line currents), as a redundant safety check.

3.2. *E-Brake*

The small actuators of Type II (28Nm) need to be especially lightweight since they are planned to be used on the robot's wrist. On the other side, current COTS safety brakes are very bulky, which would unnecessarily increase the size and weight of the small actuators. For that reason, we developed an electronic brake (E-brake). This is an additional electronic board which will be included in the 28Nm actuators and will short-circuit the motor phases in order to inhibit the movement after a shutdown or a power fail.

4. Low-level Actuator Control

4.1. *Deflection Controller*

The FPGA-based robot joint controller developed previously at DFKI (cascaded controller for position, velocity, and motor current) has been extended for the control of the spring deflection. An additional PID control loop controls the measured deflection of the spring element of the serial-elastic actuators by either acting on the velocity controller input or by directly acting on the motor current controller input (Fig. 4). A deflection controller is cascaded with a motor current controller. In addition, a joint position and velocity controller are working in the background. They are activated only in case a predefined limit of velocity or position is reached and then override the deflection controller.

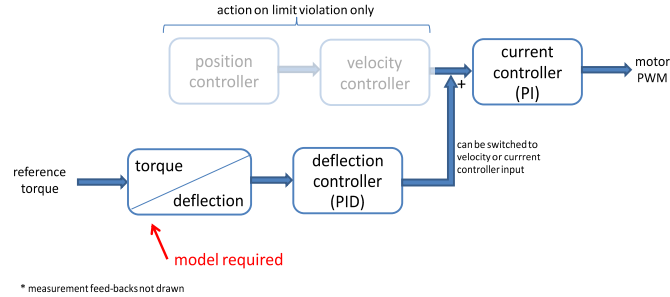


Fig. 4. Controller structure

4.2. Spring Model

The model of the spring deflection is required for controlling the actuator torque. As experimental setup to test the torque-deflection model, a load was mounted on the actuator so that the torque could be easily calculated by the Equation $\tau = m * g * r * \sin(\theta)$, where m is the mass of the load (7.25 kg), g is the gravity value and θ stands for the rotation angle of the pendulum and r represents the position vector which changes from 14 cm to 56 cm in 10 experiments.

The torque-spring deflection is modeled by using joint probability densities which are represented by a mixture of Gaussians: $P(\tau, \theta, \theta_s, \text{sign}(v))$, where τ is the actuator output torque, θ represents the rotation angle, θ_s is the spring deflection and $\text{sign}(v)$ stands for the sign of the velocity.

5. Initial Experiments

5.1. Deflection controller

Initially, experiments to determine the deflection vs. load torque relationship have been carried out. A known load is rotated by the actuator in the range of approx. ± 170 degree, while actuator positions are measured by the different sensors (before and after the mechanical spring). Since slow motions have been used, inertial properties have been ignored.

Figure 5 shows the resulting control performance when controlling the deflection. The actuator controller receives a sinusoidal deflection reference to be tracked. The top plot shows the resulting motion. At around $t=7s$, the motion is interrupted externally by hand, visible in the position plot.

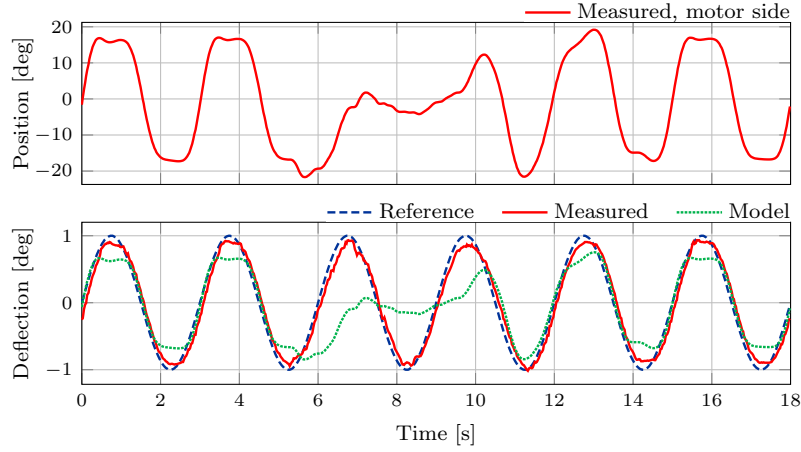


Fig. 5. Result of deflection control acting against an external disturbance. The top figure shows the position 'before' the spring (motor side). The bottom figure shows the deflection measured using the difference of position between the sensors placed before and after the spring. In red, the deflection measured; in blue, the reference deflection $x * \sin(\omega t)$; in green, the deflection according to the load torque, assuming a linear relationship

5.2. Spring model

The result of a first experiment to determine the torque vs deflection relation is shown in Figure 6 (left).

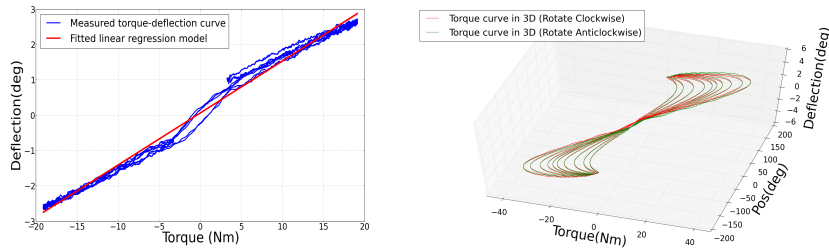


Fig. 6. Torque-spring deflection curves with 10 different load positions. *left*: A fitted linear regression model (red line): $\tau = a * \theta_s + b$ is used for representing the measured torque-spring deflection curve (blue line), where τ is the motor torque and θ_s is the deflection of the spring. *right*: The motor rotating position is used as the third dimension for training the DGMM model.

As the Figure shows, the torque-spring deflection (blue line) of the elastic spring system presented a hysteresis characteristics which is difficult to be precisely represented by a linear model (red line). Therefore, we investigate to model the torque-spring deflection by using a dynamic Gaussian

mixture model (DGMM). The model is trained by the data collected from the 10 training experiments which is shown in Figure 6(right).

For evaluating the trained model, the data from a testing experiment is used. The spring deflection, rotation angle and velocity of the motor are used as the inputs, and the actuator torque is estimated according to the Eq. $E(\tau|\theta_s, \theta, \text{sign}(v))$. The comparison of the predicted torques from the linear model and a DGMM model from the results of this offline test shows the DGMM model is able to model the elastic spring and the performance is better than a linear model.

6. Acknowledgment

The FourByThree project has received funding from the European Union's Horizon 2020 research and innovation programme, under Grant Agreement No. 637095.

References

1. S. Haddadin, A. Albu-Schffer and G. Hirzinger, Safe physical human-robot interaction: measurements, analysis and new insights, in *Robotics Research*, (Springer, 2011) pp. 395–407.
2. Rethink Robotics www.rethinkrobotics.com, [Online; accessed 22-April-2016].
3. Universal Robots www.universal-robots.com, [Online; accessed 22-April-2016].
4. KUKA LBR iiwa www.kuka-lbr-iiwa.com, [Online; accessed 22-April-2016].
5. J. Hilljegerdes, P. Kampmann, S. Bosse and F. Kirchner, Development of an intelligent joint actuator prototype for climbing and walking robots, in *International Conference on Climbing and Walking Robots (CLAWAR-09)*, 2009.
6. S. Bartsch, T. Birnschein, F. Cordes, D. Kühn, P. Kampmann, J. Hilljegerdes, S. Planthaber, M. Römmermann and F. Kirchner, SpaceClimber: Development of a six-legged climbing robot for space exploration, in *Proceedings for the Joint Conference of ISR 2010 (41st International Symposium on Robotics) and ROBOTIK 2010 (6th German Conference on Robotics)*, (VDE Verlag GmbH, June 2010).
7. M. Mallwitz, N. Will, J. Teiwes and E. A. Kirchner, The CAPIO active upper body exoskeleton and its application for teleoperation, in *Proceedings of the 13th Symposium on Advanced Space Technologies in Robotics and Automation. ESA/Estec Symposium on Advanced Space Technologies in Robotics and Automation (ASTRA-2015)*, (ESA, 2015).
8. M. Zenzes, P. Kampmann, T. Stark and M. Schilling, NDLCOM: Simple protocol for heterogeneous embedded communication networks, in *Proceedings of the Embedded World Exhibition and Conference, at Embedded World 2016, February 23-25, Nrnberg, Germany*, 2016.